COMMUNICATIONS IN NUMERICAL METHODS IN ENGINEERING
Commun. Numer. Meth. Engng 2000; **00**:1–6 *Prepared using* cnmauth.cls *[Version: 2002/09/18 v1.02]*

A node-based agglomeration AMG solver for linear elasticity in thin bodies

Prasad S. Sumant [1]*, Andreas C. Cangellaris [2] and Narayana R. Aluru [1]

[1] *Dept. of Mechanical Science and Engineering, University of Illinois 1206 W. Green St., Urbana, Illinois, 61801, U.S.A.*
[2] *Dept. of Electrical and Computer Engineering, University of Illinois 1406 W. Green St., Urbana, Illinois, 61801, U.S.A.*

SUMMARY

This paper describes the development of an efficient and accurate algebraic multigrid finite element solver for analysis of linear elasticity problems in two dimensional thin body elasticity. Such problems are commonly encountered during analysis of thin film devices in micro-electro-mechanical systems. An algebraic multigrid based on element interpolation is adopted and streamlined for the development of the proposed solver. A new, node-based agglomeration scheme is proposed for computationally efficient, aggressive and yet effective generation of coarse grids. It is demonstrated that use of appropriate finite-element discretization along with the proposed algebraic multigrid process preserves the rigid body modes that are essential for good convergence of the multigrid solution. Several case studies are taken up to validate the approach. The proposed node-based agglomeration scheme is shown to lead to development of sparse and efficient intergrid transfer operators making the overall multigrid solution process very efficient. The proposed solver is found to work very well even for Poisson's ratio > 0.4. Finally, an application of the proposed solver is demonstrated through a simulation of a micro-electro-mechanical switch. Copyright © 2000 John Wiley & Sons, Ltd.

KEY WORDS: AMGe; linear elasticity; FEM; nodal agglomeration; multigrid; MEMS

1. INTRODUCTION

A linear elasticity analysis is frequently required during simulations of multiphysics problems in applications such as micro-electro-mechanical systems (MEMS) [1]. Typically, these modern devices involve complicated geometries, extremely high aspect ratios and disparate material properties. Finite element method (FEM) is the most commonly used numerical method for their analysis [2]. However, the use of FEM discretization often leads to systems of equations that are large, sparse, ill-conditioned and semi-definite or indefinite. Many standard iterative methods, like incomplete Cholesky preconditioned conjugate gradient, break down in case

*Correspondence to: Prasad S. Sumant, Dept. of Mechanical Science and Engineering, University of Illinois 1206 W. Green St., Urbana, Illinois, 61801, U.S.A.
email: psumant2@uiuc.edu

the matrix is indefinite or semi definite. A particular example of such a case is a cantilever beam with aspect ratios (length-to-height ratio) greater than 50:1. Aspect ratios commonly encountered in MEMS structures are in the range of 50:1 to 500:1. Also, incomplete LU factorization results in relatively large number of non-zero entries in the L and U factors and thus their efficiency is not satisfactory.

Multigrid approaches offer a potentially superior alternative to these methods for the iterative solution of the FEM approximation of this class of problems. Whereas geometric multigrid methods have been used successfully for preconditioning of FEM approximations of the Laplace equation, their application is most suitable to more structured geometries [3]. In particular, their usefulness is limited when the choice of coarse grids is not obvious. Algebraic multigrid methods (AMG), on the other hand, do not rely on the attributes of the geometry under consideration but operate only on the linear system and take advantage of the nature of the algebraic error [3].

Classical AMG theory has been based on M-matrices (M-matrix is a symmetric positive definite matrix with positive entries on the diagonal and non-positive off-diagonal entries). However, as stated earlier, frequently we encounter non-M matrices in the FEM approximation of the aforementioned class of problems. For some of the problems, particularly scalar problems with one degree of freedom per node, classical AMG may still be used after careful problem-based parameter tuning. However, a systematic approach for its use is not available.

AMG-based solvers for elasticity face several challenges due to the presence of two, coupled unknowns per node in the case of two-dimensional problems and three, coupled unknowns per node in the case of three-dimensional problems. Most AMG approaches have encountered difficulties handling such problems. Griebel et al. [4] presented a generalization of classical AMG methodology for these problems through a block approach. The methodology required the a-priori definition of two parameters α and β during the set up phase, in a manner analogous to that in classical AMG. They demonstrated that interpolation is able to conserve rigid body modes for translation for all grids, while those corresponding to rotation are conserved only for point symmetric grids. For plane strain problems, they were able to demonstrate satisfactory convergence rates for Poisson's ratio up to 0.4; however, the convergence rates rapidly deteriorated for Poisson's ratio > 0.4. This is problematic for beams used in MEMS devices, since Poisson's ratio > 0.4 is commonly encountered. For example, Au electrodes have a Poisson's ratio of 0.42.

In the context of semi-definite problems in crystals with free boundaries, Xiao et al. [5] recently proposed an AMG approach in which interpolation operators are constructed to reproduce rigid body modes. Their methodology relies on the geometric information of grid coordinates. Smoothed aggregation methods were introduced by Vanek et al. [6] to tackle elasticity problems using prior knowledge of rigid body modes. In order to better approximate the smooth error, Brezina et al. [7] have proposed AMG based on element interpolation (AMGe). They make use of local stiffness matrices for defining very accurate interpolation operators. The focus in [7] is on developing a robust interpolation scheme without worrying about the choice of underlying coarse grids. Some case studies were used to demonstrate the robustness of the AMGe interpolation in conjunction with traditional coarsening strategies like geometric coarsening. In [8], a face based agglomeration algorithm is introduced to form coarse grids with an AMGe interpolation procedure used for forming the interpolation operators. A case study involving a two-grid approach on a square domain was used to demonstrate the validity of their method.

One of the important components of multigrid solution process is the formation of the coarse grid. Formation of coarse grid is dictated by several conflicting objectives, namely, set up cost, ease of set up without having to generate too much information, good convergence, sparsity, effective problem size reduction, ease of recursion and consistent coarse grid formation with sufficient coarse grid nodes for AMGe process. In the following we present a simple and effective algorithm for systematically generating coarse grids and defining coarse grid points. The proposed algorithm allows for a systematic application of the AMGe interpolation procedure. For elasticity, where multiple degrees of freedom (d.o.f) per node must be accommodated, our algorithm defines the coarse d.o.f's as the set of all d.o.f's per coarse node. So the coarsening is carried out as though it is done for a scalar problem. This avoids creation of non-physical grids. We adopt a block approach for implementing the AMGe interpolation procedure. We demonstrate that it preserves rigid body modes of translation and rotation for an appropriate finite element discretization. We demonstrate the robustness and accuracy of the proposed algorithm through a series of numerical studies that involve both structured and unstructured grids for well conditioned and ill conditioned/high aspect ratio problems. Finally, we demonstrate how the proposed node-based AMGe solver can be utilized for efficient elasticity analysis of MEMS devices.

2. FEM for elasticity

Let us a consider an elastic solid described by the domain $\Omega \subset R^2$ under the influence of different forces. The governing equations are

$$\begin{aligned} \frac{\partial \sigma_{xx}}{\partial x} + \frac{\partial \sigma_{xy}}{\partial y} &= 0 \\ \frac{\partial \sigma_{yx}}{\partial x} + \frac{\partial \sigma_{yy}}{\partial y} &= 0 \end{aligned} \tag{1}$$

where σ_{xx}, σ_{yy} are stresses normal to the x and y directions, respectively, and σ_{xy} is the shear stress. For plane strain, the stresses are related to corresponding strains as follows,

$$\left\{ \begin{array}{c} \sigma_{xx} \\ \sigma_{yy} \\ \sigma_{xy} \end{array} \right\} = \frac{E}{(1+\nu)(1-2\nu)} \left[\begin{array}{ccc} 1-\nu & \nu & 0 \\ \nu & 1-\nu & 0 \\ 0 & 0 & 1-2\nu/2 \end{array} \right] \left\{ \begin{array}{c} \epsilon_{xx} \\ \epsilon_{yy} \\ \epsilon_{xy} \end{array} \right\} \tag{2}$$

where E is the Young's modulus of elasticity and ν is the Poisson's ratio. It is immediately clear from the above expression that as ν approaches 0.5 the stress-strain relation matrix becomes increasingly ill-conditioned. All physical materials have $\nu \in [0, 0.5)$. For plane stress,

$$\left\{ \begin{array}{c} \sigma_{xx} \\ \sigma_{yy} \\ \sigma_{xy} \end{array} \right\} = \frac{E}{(1-\nu^2)} \left[\begin{array}{ccc} 1 & \nu & 0 \\ \nu & 1 & 0 \\ 0 & 0 & 1-\nu/2 \end{array} \right] \left\{ \begin{array}{c} \epsilon_{xx} \\ \epsilon_{yy} \\ \epsilon_{xy} \end{array} \right\} \tag{3}$$

Strains ϵ's are, in turn, related to displacements u, v in the x, y direction as,

$$\left\{ \begin{array}{c} \epsilon_{xx} \\ \epsilon_{yy} \\ \epsilon_{xy} \end{array} \right\} = \left\{ \begin{array}{c} \frac{\partial u}{\partial x} \\ \frac{\partial v}{\partial y} \\ \frac{\partial u}{\partial y} + \frac{\partial v}{\partial x} \end{array} \right\} \tag{4}$$

Through a weighted residual process on a finite element discretization of the domain into N nodes and N_e elements, the governing equations are approximated in terms of a system of linear equations of the form

$$Ax = b \tag{5}$$

where A is the $2N \times 2N$ stiffness matrix, x is the $2N \times 1$ displacement vector and b is the $2N \times 1$ force vector. Thus, corresponding to each node there exists a 2×1 displacement vector $[u \;\; v]^T$. The finite element discretization used utilizes either isoparametric three-node linear triangular elements or four-node bilinear quadrilateral elements. Both types of elements are complete in the sense that they are able to represent zero-strain state corresponding to rigid body modes of translation and rotation [9]. For example, let us consider the shape functions used for interpolation of nodal displacements in bilinear quadrilateral elements [9],

$$u(x) = \alpha_1 + \alpha_2 x + \alpha_3 y + \alpha_4 xy \tag{6}$$

$$v(x) = \beta_1 + \beta_2 x + \beta_3 y + \beta_4 xy \tag{7}$$

A non-zero α_1 (with the rest of the coefficients all zero) gives rigid body mode in x, a non-zero β_1 (with the rest of the coefficients all zero) gives rigid body mode in y, and $\alpha_3 = -\beta_2$ gives rigid body rotation. This property is important for ensuring a convergent finite element solution. Consequently, the global stiffness matrix assembled from such a discretization without boundary conditions is singular and its null space, $N(A)$, consists of the rigid body modes of horizontal and vertical translation and in-plane rotation. If the rows and columns in the matrix A (without the boundary conditions) are rearranged such that all variables corresponding to horizontal displacements u are first, followed by vertical displacements v, we have for $N(A)$

$$\begin{bmatrix} A_{uu} & A_{uv} \\ A_{vu} & A_{vv} \end{bmatrix} \begin{bmatrix} u \\ v \end{bmatrix} = 0 \tag{8}$$

This null space is spanned by

$$N(A) = span\left\{(1,0)^T, (0,1)^T, (-y,x)^T\right\} \tag{9}$$

where, $1 = (1,1,...,1)^T$, $0 = (0,0,...,0)^T$, $y = (y_1, y_2, ..., y_N)$ and $x = (x_1, x_2, ..., x_N)$.

3. Numerical solution through AMG

Iterative solvers like Gauss-Seidel when applied to the solution of $Ax = b$ exhibit slow convergence, especially for problems involving significant material and geometric complexity. This can be attributed to their inability to reduce the smooth components of the error effectively. Multigrid methods offer a remedy to this problem.

Multigrid methods work on the principle that the smooth components appear oscillatory on a coarser grid, and thus can be effectively reduced on the coarser grid through smoothing. Consequently, they utilize a hierarchy of grids of variable spatial resolution, and require the transfer of the residual error in the iterative solution of the problem from one grid to another. For our purposes, AMG is employed to improve the performance of the Gauss-Seidel smoother.

The basic algorithm for a V-cycle V(ν_1,ν_2,x,b) AMG is outlined below [3]

Algorithm 1. V-cycle AMG

IF (Current Grid is not the Coarsest Grid),

(1.1) Relax $Ax = b$ on current (fine) grid (using iterative solver like Gauss-Seidel) for ν_1 times.
(1.2) Compute residual on current (fine) grid, $r^f = b - Ax$.
(1.3) Project residual to next coarse grid using *restriction* operator R, $r^c = Rr^f$.
(1.4) Set $x^c = 0$ and call $V^c(\nu_1, \nu_2, x^c, r^c)$
(1.5) Interpolate error back to the fine grid using *interpolation* operator P, $e^f = Pe^c$.
(1.6) Correct the solution on the fine grid $x \leftarrow x + e^f$.
(1.7) Relax on the fine grid for ν_2 times.

Else
(1.8) Compute $A_c = P^T AP$ and solve the equation $A_c e^c = r^c$ exactly on the coarsest grid.

Implementation of the above algorithm requires the following:

- Development of coarse grid(s) at multiple levels - defining new elements and nodes
- Definition of the restriction and interpolation operators (R, P) and the matrix A_c for the coarse grid.

Its computational cost is dictated by

- Set up cost: Cost of forming coarse grids, interpolation (or restriction) operators, coarse grid matrices (A_c)
- Execution cost: Cost of performing V cycles to achieve desired tolerance. It depends on residual reduction obtained in each cycle and the sparsity of intergrid and coarse grid operators.

The success of AMG depends on the accuracy with which smooth components of the error can be represented on the coarse grid, which, in turn, depends on the interpolation and restriction operators. In classical AMG, these operators are obtained using certain rules that are based solely on the relative magnitudes of the matrix entries (notion of strength of connection) without regard to underlying physics. This approach is suitable for systems of equations involving M-matrices where the strength of connection is easy to measure. Also, the strength of connection is based on a predefined parameter, which may have to be changed from problem to problem. However, in systems involving non M-matrices or systems representing complex material and geometric domains, a different approach needs to be adopted for effective construction of these components.

This is the main motivation for the development of AMG based on element interpolation (AMGe) [7]. It makes use of information contained in element stiffness matrices for building multigrid components, while at the same time does not rely on grid geometry or definition of any problem-specific parameter. The development of such a solver is described next.

4. AMGe based on nodal agglomeration

4.1. Node-based agglomeration for coarse grids

Any standard mesh generator gives information about node numbering, element numbering, and the nodes associated with a given element. Thus, for the sake of efficiency, it is desirable to use only this information for forming coarse grids. This is accomplished through a node-based agglomeration process as described next.

We begin by defining the following:
Boundary $B = \{n_1, ..., n_b\}$, i.e. a collection of nodes
Element $e = \{n_1, ..., n_p\}$, i.e. a collection of p nodes, obtained from the mesh generator
Agglomeration - The process of combining fine elements into a single coarse element. Each node is assigned an integer weight, w. Agglomeration is controlled using the weight assigned to a node.

Algorithm 2. Node-based Agglomeration

- **Initialization:** Set $w(n) = 0$ for all nodes n.
- **Loop over all nodes**
  For $n = 1, \text{NumberofNodes}$

  1. If $w(n) = -1$, increment n and go to the next node
     Else
     Set $E = e_1 \cup e_2 ..... \cup e_m$, where $e_1, e_2, ...e_m$ are the elements to which the node n belongs. Thus, combine all elements connected to a node into a single agglomerated element.
  2. Set $w(k) = -1$, for all nodes k contained in the elements that have been agglomerated.

- **Sweep over the left-over elements**
  For all elements that have not been agglomerated,

  1. For all nodes k on this element, determine the agglomerated element E to which each node belongs
  2. If more than one node belong to the same agglomerate, choose that agglomerate to merge the current element with. Otherwise, just add the current element to an agglomerate corresponding to any one node.

The above agglomeration algorithm results in the formation of a coarser grid consisting of agglomerated elements. The complexity of this algorithm is linear ($O(N)$). This algorithm makes sure that no fine element is part of more than one agglomerate.

The next task involves choosing the nodes that will be retained on the coarse grid. The choice of these nodes, which will be referred to as *coarse nodes*, will dictate the accuracy with which interpolation operators between the coarse and fine grids are built. The coarse nodes are defined as follows. Intersection of three or more agglomerated elements is considered as a coarse node. The boundary of the domain is treated as one agglomerated element. Thus, for each node that is not on the boundary in the fine grid, we find the number of agglomerated

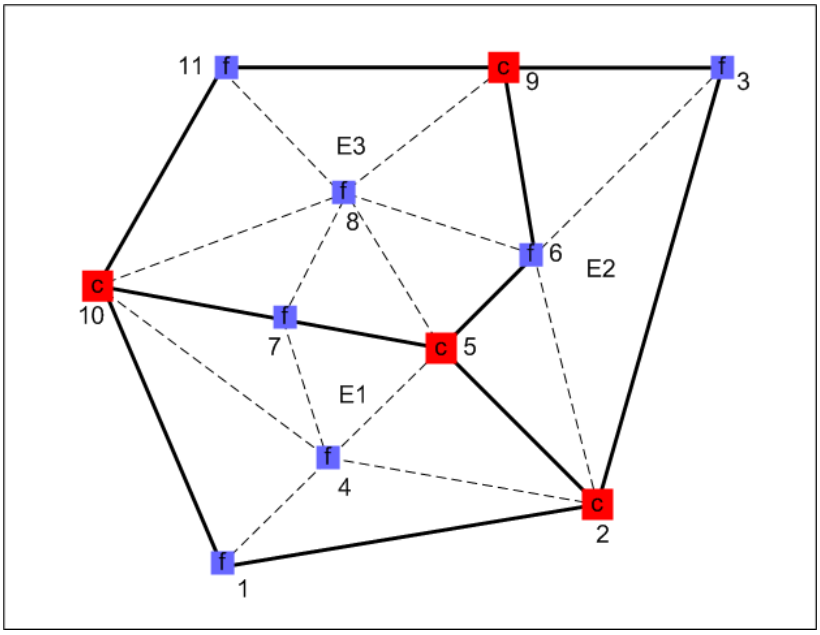

Figure 1. Node-based agglomeration - definition of coarse and fine nodes.

elements that contain this node. If the number is at least 3, then this node is identified as a coarse node. If a fine node is on the boundary, then it is defined as a coarse node if it is shared by at least 2 agglomerated elements. Since for elasticity problem we have 2 d.o.f's per node, all d.o.f's at a node are considered as coarse d.o.f's. Finally, for a coarse element we consider the agglomerated element after dropping the fine nodes present in that agglomerate.

The aforementioned algorithm is easy to implement recursively. Furthermore, because of its node-centric nature, it results in very aggressive coarsening. Examples justifying this statement are presented in the numerical studies section.

An illustration of the node-based agglomeration process is depicted in Figure 1. Dotted lines mark fine grid triangular elements. There are three agglomerates, namely, E1, E2 and E3. Nodes 2, 5, 9, 10 are coarse nodes. Nodes 1, 3, 4, 6, 7, 8, 11 are fine nodes. Thus, E1 with 2,5,10 is one coarse element; E2 has 2,5,9; while E3 has 5,9,10.

Implementation of this algorithm recursively on an unstructured triangular grid (generated using Triangle [10]) results in the formation of successively coarser grids as depicted pictorially in Figure 2.

4.2. Formation of the intergrid transfer operators and the coarse matrix A_c

As mentioned earlier, the success of AMGe depends on the accuracy with which the residual error from the fine grid is mapped onto the coarse grid for subsequent smoothing. A set of rules involving element stiffness matrices has been proposed and justified in [8] for this mapping. These rules constitute the foundation for an algorithm for the construction of the prolongation operator P and the restriction operator R. It is noted that the two operators are related by

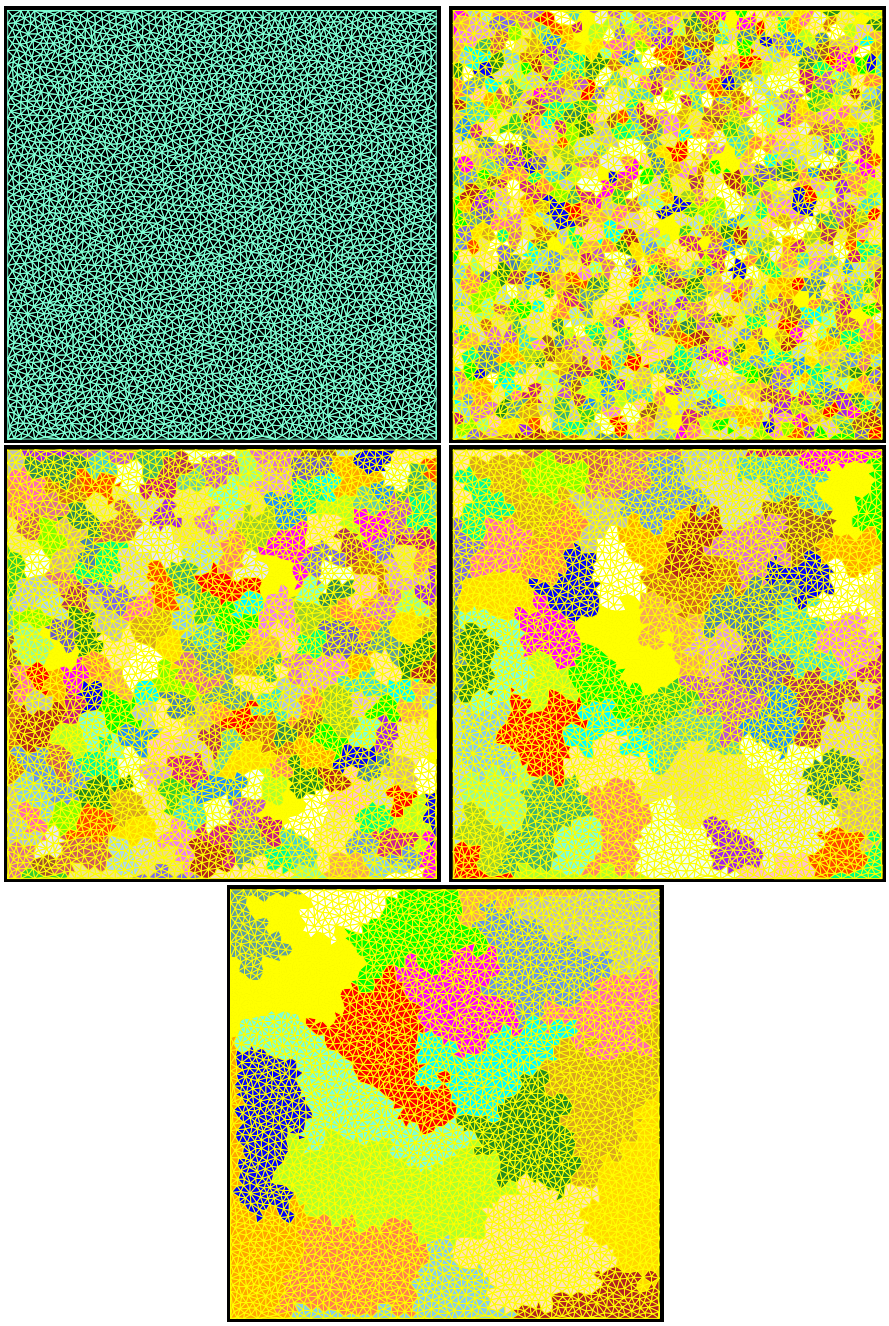

Figure 2. Multiple coarse grids resulting from the recursive implementation of the node-based agglomeration algorithm (Algorithm 2).

[8]

$$R = P^T \tag{10}$$

Thus, construction of only one of the two matrices is required. The algorithm described below is for the construction of the prolongation matrix P.

Algorithm 3. Construction of Prolongation Matrix
If a node n is a coarse node then the interpolation is identity.
Else the following sets are formed:

- A neighborhood $\Omega(n) = \cup$ { all agglomerated elements $E(n)$ that contain n }.
- A set $N(n) = \cap${ all agglomerated elements $E(n)$ that contain n }.
- Boundary, $\partial N(n)$, of the set $N(n)$. $\partial N(n)$ includes the nodes in $N(n)$ that are coarse.

The coarse nodes $n_c^1, ..., n_c^p$, contained in the set $\partial N(n)$, are used for interpolation. For example, for node 6 in Fig. 1, neighborhood $\Omega(n) = E2 \cup E3 = \{2, 3, 5, 7, 8, 9, 10, 11\}$, set $N(n) = \{5, 6, 9\}$ and $\partial N = \{5, 9\}$. A matrix, $A_{\Omega(n)}$, is assembled using stiffness matrices of all elements contained in the neighborhood. The matrix is subsequently divided into a two-by-two block structure, corresponding to the partitioning $(\Omega(n) \backslash \partial N(n)) \cup \partial N(n)$, as follows

$$A_{\Omega(n)} = \begin{pmatrix} A_{ii} & A_{ib} \\ A_{bi} & A_{bb} \end{pmatrix} \tag{11}$$

In the above, the subscript i stands for interior nodes, $i \in (\Omega(n) \backslash \partial N(n))$ ($\{2, 3, 7, 8, 10, 11\}$ in above example) , and b stands for boundary nodes, $b \in \partial N(n)$ ($\{5, 9\}$ in above example). This definition makes the interpolation operator constructed in this fashion compatible.

It is important to note that A_{ii} is $2N_i \times 2N_i$, A_{ib} is $2N_i \times 2N_b$, A_{bi} is $2N_b \times 2N_i$ and A_{bi} is $2N_b \times 2N_b$. This approach, where the entries corresponding to horizontal and vertical displacements at a node are considered in a block fashion, is important to ensure the conservation of rigid body modes. It is also known as the block approach. The interpolation (prolongation) coefficients for the node n under consideration are obtained by extracting the n^{th} row of the following product [8]

$$C = -A_{ii}^{-1} A_{ib} \tag{12}$$

Once the prolongation matrix has been developed stiffness matrices for each coarse grid element can be formed by first extracting the interpolation operator, P^e, for the nodes contained in that element. Then, the stiffness matrix for the coarse grid element is computed as

$$A_c^e = P^{eT} A_{\Omega(n)} P^e \tag{13}$$

Finally, the coarse grid global stiffness matrix, A_c, is obtained from the assembly of all coarse grid element stiffness matrices.

This completes all the components that are necessary for the application of AMG.

4.3. Preservation of rigid body modes

Let us consider the assembled neighborhood matrix A_Ω. Let $x = [x_i \;\; x_b]^T$ be a vector in the null-space of A_Ω. As stated earlier, if the finite element discretization consists of three-node

linear triangular elements or four-node bilinear quadrilateral elements, and if a complete linear polynomial is used for interpolation, then it can be shown that the element can represent zero-strain state or rigid body modes corresponding to translation and rotation. Since the neighborhood matrix A_Ω locally is an assembly of stiffness matrices in the neighborhood, x corresponds to the local rigid body mode. Next, consider a block partitioning of the neighborhood matrix,

$$A_\Omega = \begin{pmatrix} A_{ii} & A_{ib} \\ A_{bi} & A_{bb} \end{pmatrix} \tag{14}$$

So, the rigid body modes locally satisfy,

$$\begin{bmatrix} A_{ii} & A_{ib} \\ A_{bi} & A_{bb} \end{bmatrix} \begin{bmatrix} x_i \\ x_b \end{bmatrix} = 0 \tag{15}$$

Thus, we have

$$A_{ii}x_i + A_{ib}x_b = 0 \tag{16}$$

which leads to

$$x_i = -A_{ii}^{-1}A_{ib}x_b \tag{17}$$

A comparison of this with the equation for interpolation reveals that interpolation preserves the rigid body modes locally. Furthermore, a d.o.f at a fine grid point is interpolated only from the coarse grid points in its neighborhood. Thus, the rigid body modes are conserved even globally.

5. NUMERICAL SIMULATIONS

In this section we present several case studies aimed at the demonstration and validation of the proposed AMGe solver. A variety of metrics are used for assessing the performance of our proposed solver. We define relative residual at the mth iteration as,

$$rel.\ res = \frac{\|r_m\|_{l_2}}{\|r_0\|_{l_2}} \tag{18}$$

The AMG iterations are stopped when

$$rel.\ res \leq tol \tag{19}$$

The *tol* is taken as 1e-6 for most of the case studies. The asymptotic convergence factor ρ is defined as

$$\rho = (rel.res_{iter})^{1/iter} \tag{20}$$

In order to quantify the performance of coarsening process, we compute the *total-grid-complexity*, $c(G)$, as follows,

$$c(G) := \sum_{i=0}^{J-1} n_u^i / n_u^0 \tag{21}$$

where n_u^i is the number of grid points of the ith level and J is the total number of levels. The computational cost of each AMG cycle is dictated by the non-zero entries in the grid operator

matrix A at each coarse grid level. To estimate this, we define the *total-operator-complexity*, $c(A)$, as follows,

$$c(A) := \sum_{i=0}^{J-1} nnz^i / nnz^0 \tag{22}$$

where nnz^i is the number of non-zeros of the grid operator at the ith level.

We consider two main classes of problems, square plate discretized using both structured and unstructured grids, and a cantilever beam discretized using a structured grid.

5.1. Unit square

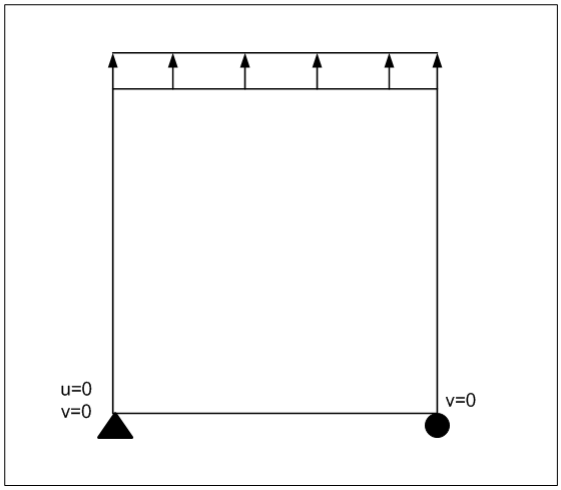

Figure 3. Unit square

As a first case study we consider the problem examined in [5] (Figure 3). It utilizes an unstructured triangular grid on a unit square and plane strain elasticity formulation. Relative residual stopping criterion is 1e-6. Triangle [10], is used for generation of unstructured grids for our simulation. V(3,3) AMG cycles are used. Summarized in table I is a comparison of number of iterations for convergence between our solver for different levels of grid and the method in [5] for two extreme grid sizes. It is evident that the performance of our solver gets even better for finer grids.

# elements	ref[5]	our solver - 2 level	our solver - 3 level	our solver - 4 level
1230	12	5-6	9	11-12
57566	10	4	5	6-7

Table I. Unit square: Unstructured triangular grid

Next, we consider the problem given in [8]. In that paper, a face-based agglomeration process, called topology algorithm, was introduced. Structured grids with bilinear quadrilateral elements were used for discretization of the unit square domain (Figure 3). Four different grid

Grid #		1	2	3	4
# fine elements	ref[8]	400	900	1600	2500
	our solver	400	900	1600	2500
# coarse elements	ref[8]	118	253	438	673
	our solver	121	256	441	676
# fine dofs	ref[8]	882	1922	3362	5202
	our solver	882	1922	3362	5202
# coarse dofs	ref[8]	314	624	1034	1544
	our solver	280	570	960	1450
# iterations	ref[8]	9	9	9	9
	our solver	7-8	7-8	7-8	7-8

Table II. Unit square with structured rectangular grid: two-level AMG

sizes were considered with the relative residual stopping criterion set at 1e-6. The solution was obtained using two-level V(1,1) AMGe cycles. Table II gives a comparison between the results in [8] and the proposed solver. There is a very good agreement between their results and ours, both in terms of coarsening and convergence rate. This comparison establishes the validity of the proposed node-based agglomeration process. It is important to stress that the node-based agglomeration process achieves the same performance without having to generate extra information about faces as required by the face-based agglomeration algorithm.

The next study deals with the problem considered in [4]. For the purpose of this study, the relative residual reduction stopping criterion is taken to be 1e-12, same with the one used in [4]. The problem considered involves the application of a multi-level AMG algorithm for a structured rectangular grid on a unit square for three different individual cell sizes. Both V(1,1) and V(3,3) cycles are used along with two different levels for our solver. A variety of performance parameters, grid complexity, c(G), operator complexity, c(A), and convergence factor are compared in table III. It is evident from the comparisons that our solver exhibits very good performance. It is noted that as we increase the level of grids from 3 to 4 there is no significant change in c(A) and c(G). In fact their values remain considerably lower than 2. This is important since these complexities dictate the cost of each V cycle. Their small values indicate that the nodal agglomeration coarsening process used is able to maintain good sparsity both in the intergrid transfer operators and the coarse grid operators. Thus, the computation of the V cycles in our algorithm is very efficient. Based on our numerical experiments, use of three or four levels of grids is sufficient for obtaining the desired performance.

	ref [4]			our solver - 3 level				our solver - 4 level			
h	c(A)	c(G)	ρ	c(A)	c(G)	ρ V(3,3)	ρ V(1,1)	c(A)	c(G)	ρ V(3,3)	ρ V(1,1)
1/32	2.61	1.69	0.21	1.38	1.39	0.072	0.22	1.42	1.43	0.14	0.28
1/64	2.69	1.68	0.22	1.37	1.35	0.079	0.22	1.37	1.38	0.16	0.29
1/128	2.75	1.68	0.23	1.33	1.33	0.084	0.22	1.36	1.35	0.17	0.29

Table III. Unit square with structured rectangular grid: multi-level AMG

Finally, we consider the robustness of our solver with respect to Poisson's ratio. We consider the same problem as above (i.e. plane strain on unit square) with $h = 1/128$ and Poisson's

ratio varying between 0.1 and 0.45. As pointed out earlier, in some of the MEMS structures it is common to encounter beams with a Poisson's ratio of 0.4 or greater. The asymptotic convergence factor is plotted in Figure 4. It is found to remain less than 0.35 even for Poisson's ratio greater than 0.4.

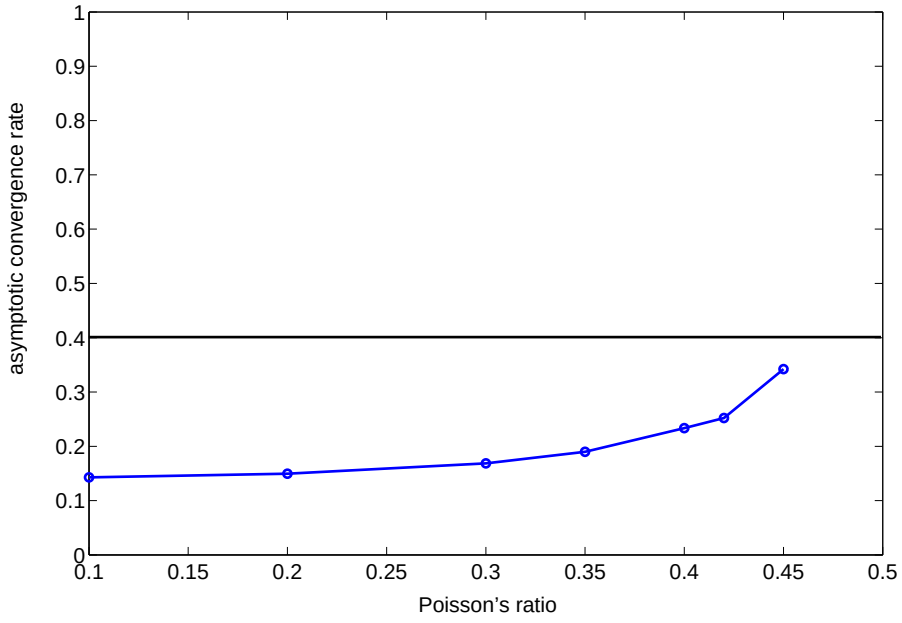

Figure 4. Unit square: Asymptotic convergence rate for different values of Poisson's ratio

5.2. Cantilever beam

In this section, we consider the application of the proposed algorithm to a generic cantilever geometry. Such structures are commonly encountered in MEMS devices. As a first example,we consider the case study given in [7]. A cantilever beam as shown in Figure 5 is considered. The length/height ratio (aspect ratio) is varied between 16:1 to 64:1. Note that as the aspect ratio increases the matrix becomes more badly conditioned and poses more challenges to the AMG algorithm. A relative residual stopping criterion of 1e-6 is used for the iterative solution. The cantilever beam is discretized using bilinear square elements. Analysis is done for plane stress with Poisson's ratio of 4/7. Both two-level and multi-level multigrid are used. For the purpose of even comparison with [7], V(0,1) cycles are used. Summarized in Tables IV and V is a comparison for two-level multigrid and multilevel multigrid. In these tables, GMG stands for geometric multigrid while AMGe stands for AMGe interpolation procedures applied using geometric coarsening strategies. From the results in the tables it becomes evident that the node-based agglomeration process in conjunction with AMGe interpolation results in very accurate solution. In fact, even for this structured grid, the performance of our solver is superior to GMG. Finally, we note that a much better performance can be achieved if V(1,1) or V(3,3)

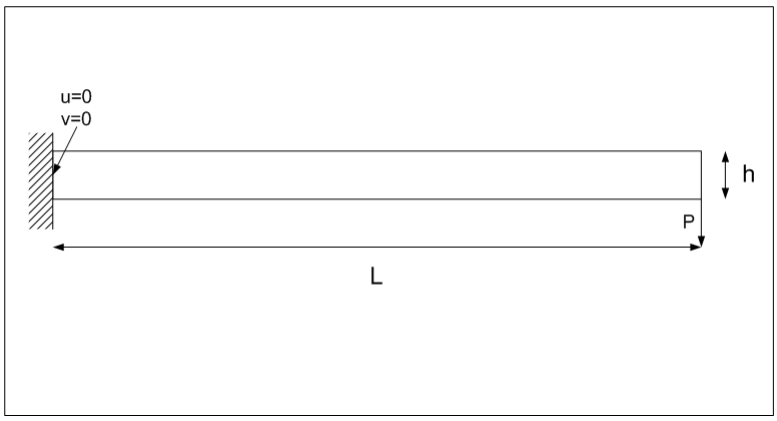

Figure 5. Cantilever problem

cycles are used instead.

Length/height	GMG	AMGe	Our solver
16	0.46	0.49	0.32
32	0.53	0.45	0.35
64	0.67	0.39	0.38

Table IV. Cantilever: Asymptotic convergence factors for two-level multigrid

Length/height	GMG	AMGe	Our solver: three-level	Our solver: four-level
16	0.77	0.58	0.34	0.46
32	0.75	0.51	0.37	0.45
64	0.67	0.39	0.40	0.48

Table V. Cantilever : Asymptotic convergence factors for multi-level multigrid

Next we consider the application of our algorithm to the solution to the problem for aspect ratios of 128:1 and 375:1 in the cantilever beam, representative of those encountered in MEMS devices. For such large aspect ratios, the resulting stiffness matrix is not positive definite and is very ill-conditioned. V(3,3) cycles and three-level multigrid are used. Table VI summarizes the results. We note that the operator and grid complexity are less than 2, independently of the aspect ratio. Also, the convergence rate remains very good (< 0.3) even at an aspect ratio of 375:1.

6. Practical application to an RF MEMS switch

In this section, we describe the application of the proposed solver pertinent to the modeling of a MEMS device, namely, a simply supported RF MEMS capacitive switch [11]. The cross-

Length/height	ρ	c(A)	c(G)
128	0.1950	1.73	1.65
375	0.2430	1.73	1.65

Table VI. Thin cantilever beams in MEMS

sectional geometry involved in the modeling is depicted in Figure 6. It consists of a Au beam, which is used as the top movable electrode, attached to metal posts on either side. The beam is placed over a center ground conductor, which remains fixed and serves as the ground electrode for the capacitive switch. A Si_3N_4 layer is placed on top of this electrode. The ground electrode and supporting metal posts for the top electrode are placed over a SiO_2 layer, which sits on top of a silicon substrate.

The dimensions of the structure are as follows: the length of the top electrode, L, is 300μm, its thickness, t, is 0.8μm, and its width, b, is 80 μm. The width, W, of the lower electrode is 100 μm, and its thickness, t_e, is 0.8μm. The distance between the bottom of the top electrode and the silicon nitride layer is 3 μm. The thickness of the Si_3N_4 layer, t_d, is 0.15 μm, while the thickness of the SiO_2 layer, t_{ox}, is 0.4 μm. The Si_3N_4 and SiO_2 dielectric layers have relative dielectric constants of 7.6 and 3.9 respectively. For the Au beam, the Young's modulus, E, is 80 GPa and Poisson's ratio ν is 0.42.

One of the tasks in the MEMS design process involves characterization of the electro-mechanical behavior of the switch for different voltages. For a given applied voltage, an electrostatic force acts on the top, simply supported beam, due to which the beam bends by a certain amount. The deflection of the center of the beam versus the applied voltage is usually a metric of interest to the assessment of the performance of the capacitive switch.

Electro-mechanical analysis is done using a relaxation algorithm as follows:
repeat

1. Do mechanical analysis (on the undeformed geometry) to compute structural displacements
2. Update the geometry of the movable electrode using computed displacements
3. Compute the electric field by electrostatic analysis (deformed geometry)
4. Compute electrostatic forces on the movable membrane in the deformed configuration
5. Transform the electrostatic forces to the original undeformed configuration
   until an equilibrium state is reached.

Thus, two separate analyses need to be performed : mechanical (elasticity) analysis, which is typically done using a finite element solver[2] and an electrostatic analysis, which is typically done using either a boundary element solver [2] or a finite element solver [12]. In this paper we are concerned with the finite element-based mechanical analysis. In terms of numerical linear algebra, during each step of the relaxation, we are solving a linear system of equations of the form,

$$A_m x_m = b \tag{23}$$

where A_m is a stiffness matrix associated with the top slender electrode, x_m is its displacement at the mth relaxation step and b_m is the right-hand side at the mth step. The stiffness matrix, A_m, does not change at each step. So essentially, at each step, we can update x_m as follows,

$$x_{m+1} = x_m + A_m^{-1} b_m \tag{24}$$

Also, x_m at the previous iteration step forms a good initial guess for x_{m+1} at the next step.

So our proposed node-based AMGe solver can be very efficiently used for this process. Since the grid does not change, the set up phase is carried out only once. Once the intergrid transfer operators and the coarse grid operators are ready, they are used in the V cycles in conjunction with a good initial guess to obtain very fast convergence.

For the RF MEMS capacitive switch under consideration, it is noted that the aspect ratio is 375:1 and the Poisson's ratio is 0.42. Since the membrane width (80 μm) is much larger than its thickness (0.8 μm), we perform a 2D analysis using plain strain formulation. Thus the problem poses several challenges for its solution. Our proposed solver was applied to the above problem for different voltages of values ranging between 0 V and 19 V. For each voltage, the aforementioned relaxation procedure is performed to obtain the center deflection of the top electrode. Results are compared with those obtained using ANSYS in Figure 7. There is a very good agreement in the results. Note that we employ a three-level AMG with V(3,3) cycles and 1e-6 as the stopping criterion. The grid and operator summary can be found in Table VII. The number of degrees of freedom on the coarsest grid is almost 1/7th of that on the finest grid. It is noted that for the first relaxation step we employ twenty cycles and reduce the number of V cycles at each subsequent relaxation step by 2. We observe that this process yields the same convergence with the one where twenty cycles are used for all relaxation steps. Thus, we conclude that using the previous solution as initial guess for the next step greatly accelerates convergence and reduces significantly the overall cost of the solution process. In fact, we note that if the center deflection versus applied voltage is to be obtained, a very efficient way to do it would be to begin with low voltage, and gradually increase it until the maximum desired voltage is reached. For each voltage, we can use the solution obtained from the previous lower voltage as an initial guess. Furthermore, we note that the same multigrid operators are used for each voltage. This way the overall design characterization task is carried out very efficiently.

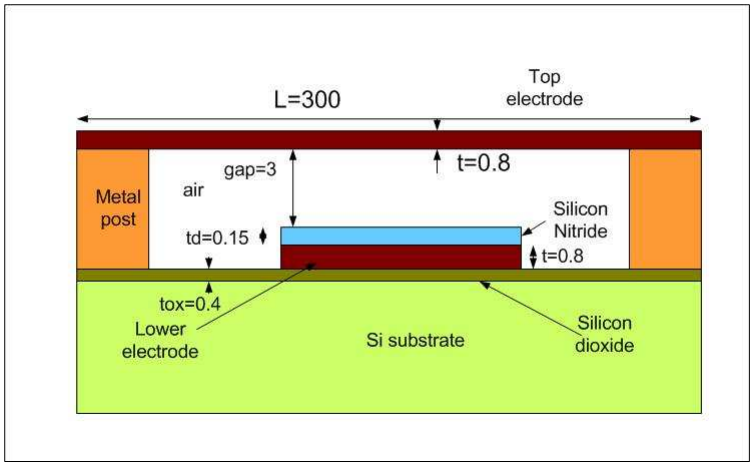

Figure 6. RF MEMS switch

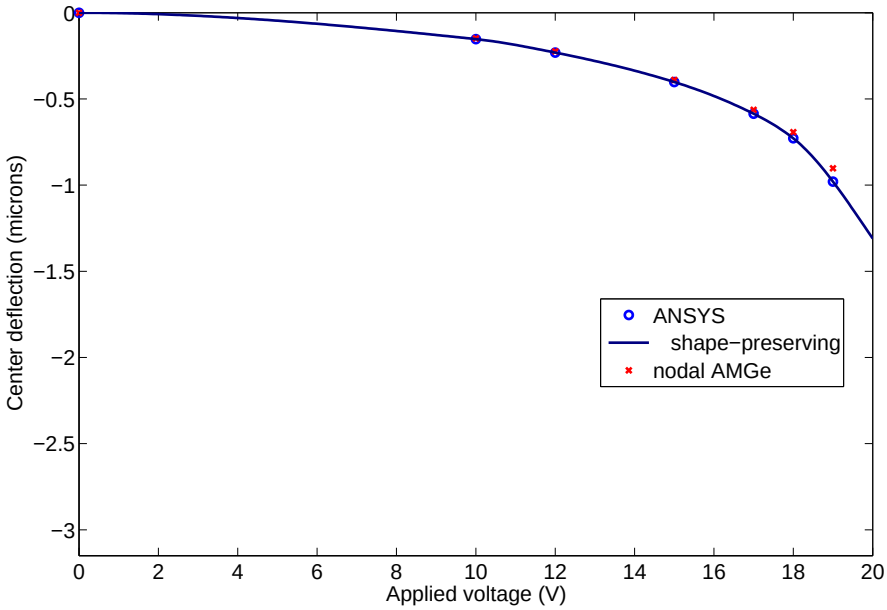

Figure 7. Center deflection : comparison between ANSYS and the proposed nodal AMGe solver

Grid	nnz(A)	# elements	# nodes
0	312052	8000	10005
1	120048	3003	4004
2	109944	1002	2502
3	75832	501	1500

Table VII. RF MEMS switch : Grid and Operator summary

7. SUMMARY

We have described the development of a nodal agglomeration-based AMGe solver for the accurate analysis of thin body elasticity. In particular, we have proposed a node-based agglomeration process that allows for a systematic application of the AMGe interpolation procedure described in [7]. The proposed agglomeration process treats the degrees of freedom at a given node in a block fashion. Thus, the coarsening in this elasticity problem is done as if it were done on a scalar problem. This ensures that non-physical coarse grids are not created. Also, the agglomeration process uses only the basic information available from a mesh generator. Its node-centric nature makes it very aggressive in terms of coarsening. We have also demonstrated that use of a complete and consistent formulation for a finite element discretization ensures conservation of rigid body modes if the AMGe interpolation procedure is applied in a block fashion.

Several case studies are taken up to demonstrate the efficiency and accuracy of our proposed solver. In particular, we have demonstrated that operator and grid complexities c(A) and c(G) are maintained low (< 2) while achieving good convergence rates of less than 0.3 for most problems. We have also demonstrated that the proposed solver delivers convergence rates of less than 0.35 even for Poisson's ratios > 0.4. For most cases considered, using two or three coarse grids was found to work very well. If two coarse grids are used, the number of degrees of freedom is reduced by approximately a factor of seven. Finally, we have presented an application of the proposed nodal agglomeration-based AMGe solver in the computer-aided design characterization of an RF MEMS capacitive switch.

ACKNOWLEDGEMENTS

This research was supported by the Defense Advance Research Programs Agency (DARPA) under Grant HR0011-06-1-0046.

REFERENCES

1. Senturia S., Aluru N., White J. Simulating the behavior of MEMS devices: Computational methods and needs *IEEE Computational Science and Engineering* 1997; **4**(1):30–43.
2. Senturia S., Harris R. , Johnson B. , Songmin K. , Nabors K. , Shulman M. , White J. A computer-aided design system for microelectromechanical systems (MEMCAD) *Journal of Microelectromechanical systems* 1992; **1**():3–13.
3. Briggs W. L., Henson V. E., McCormick S. F. *A Multigrid Tutorial* (2nd edn). SIAM: Philadelphia, 2000
4. Griebel M., Oeltz D., Schweitzer M. An algebraic multigrid method for linear elasticity *SIAM Journal of Scientific Computing* 2003; **25**(2):385–407.
5. Xiao Y., Zhang P. , Shu S. An algebraic multigrid method with interpolation reproducing rigid body modes for semi-definite problems in two-dimensional linear elasticity *Journal of computational and applied mathematics* 2007; **200**:637–652.
6. Vanek P., Mandel J., Brezina M. Algebraic multigrid by smoothed aggregation for second and fourth order elliptic problems *Computing* 1996; **56**():179–196.
7. Brezina M., Cleary A., Falgout R., Henson V. ,Jones J., Manteueffel T., McCormick S., Ruge J.W. Algebraic multigrid based on element interpolation (AMGe) *SIAM Journal of Scientific Computing* 2000; **22**(5):1570–1592.
8. Jones J., Vassilevski P. AMGe based on element agglomeration *SIAM Journal of Scientific Computing* 2001; **23**(1):109–133.
9. Bathe K. *Finite Element Procedures* (6th edn). Prentice-Hall of India 2002
10. Triangle : A two-dimensional quality mesh generator and Delaunay triangulator. http://www.cs.cmu.edu/ quake/triangle.html [10 June 2007].
11. Hamad E., Omar A. An improved two-dimensional coupled electrostatic-mechanical model for RF MEMS switches *Journal of Micromechanics and Microengineering* 2006; **16**():1424–1429.
12. Zhulin V., Owen S., Ostergaard D. Finite Element Based Electrostatic-Structural Coupled Analysis with Automated Mesh Morphing *International Conference on Modeling and Simulation of Microsystems* 2000 ():501–504.